Title
Projections between visual cortex and pulvinar in the rat

Journal
The Journal of Comparative Neurology, 529(1)

ISSN
1550-7149

Authors
Scholl, Leo R
Foik, Andrzej T
Lyon, David C

Publication Date
2021

DOI
10.1002/cne.24937

Peer reviewed

Published in final edited form as:

J Comp Neurol. 2021 January ; 529(1): 129–140. doi:10.1002/cne.24937.

Projections between visual cortex and pulvinar in the rat

Leo R. Scholl[1,2], **Andrzej T. Foik**[2], **David C. Lyon**[2,*]

[1]Department of Cognitive Sciences, School of Social Sciences, University of California, Irvine

[2]Department of Anatomy and Neurobiology, School of Medicine, University of California, Irvine

Abstract

The extrageniculate visual pathway, which carries visual information from the retina through the superficial layers of the superior colliculus and the pulvinar, is poorly understood. The pulvinar is thought to modulate information flow between cortical areas, and has been implicated in cognitive tasks like directing visually guided actions. In order to better understand the underlying circuitry, we performed retrograde injections of modified rabies virus in the visual cortex and pulvinar of the Long-Evans rat. We found a relatively small population of cells projecting to primary visual cortex (V1), compared to a much larger population projecting to higher visual cortex. Reciprocal corticothalamic projections showed a similar result, implying that pulvinar does not play as big a role in directly modulating rodent V1 activity as previously thought.

Graphical Abstract

Unlike the geniculocortical pathway which interconnects only between the lateral geniculate nucleus and primary visual cortex (V1), the pulvinar has long been known to interconnect with most if not all of visual cortex. Here we show that pulvinar interconnectivity is actually more dominant with higher visual cortex (V2) than with V1. Thus, the pulvinocortical pathway does not likely play as big a role in directly modulating V1 activity as previously thought.

[*]Corresponding author: David C. Lyon, 317B Med Surge II, University of California, Irvine, CA 92697-1275, Phone: 949-824-0447, dclyon@uci.edu.

Data Availability Statement: The data that support the findings of this study are available from the corresponding author [DCL] upon reasonable request.

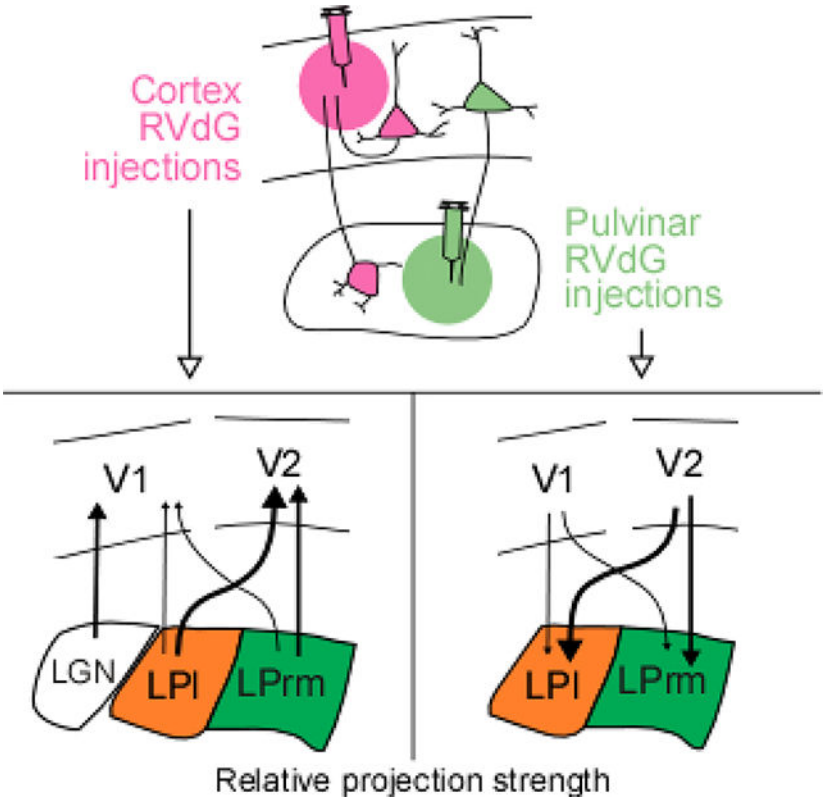

Keywords

pulvinar; lateral posterior thalamic nucleus; thalamus; visual cortex; extrageniculate pathway; rabies virus; rat; RRID:RGD_2308852; RRID:CVCL_1915; RRID:Addgene_32633; RRID:AB_2307445

Most visual information in primary visual cortex (V1) is delivered from the retina via the lateral geniculate nucleus (LGN; Jones, 1985). However, the extrageniculate visual pathway, which carries information from the retina through the superficial layers of the superior colliculus (SC) and the pulvinar (Kaas and Huerta, 1988; Stepniewska, 2003; Lyon et al., 2010), also makes major contributions to visual processing, having been implicated in gating or driving visual cortex activity both in primates (Purushothaman et al., 2012; Zhou et al., 2016) and in rodents (Tohmi et al., 2014). In comparison to the LGN, less is known about the structure and function of the extrageniculate thalamic nuclei, yet these structures have a big impact on cognition and behavior. Early behavioral studies in primates identified cells in the pulvinar that are enhanced by shifts in gaze (Petersen et al., 1985; Robinson et al., 1986; Bender, 1982), leading many to think the pulvinar is involved in directing spatial attention. Modern theories of pulvinar's role in attention include its driving of salience-based selection (Mizzi & Michael, 2014; Veale et al., 2016), guiding visual actions (Wilke et al., 2010; Zhou, Masterson, et al., 2017), and providing contextual information to visual cortex (Wilke et al., 2009; Roth et al., 2015; Jaramillo et al., 2019).

The rat pulvinar, also called the lateral posterior nucleus (LP), consists of three highly-conserved subregions based on cytoarchitecture and connectivity: caudomedial (LPcm), lateral (LPl), and rostromedial (LPrm) pulvinar (Takahashi, 1985; Nakamura et al., 2015; see Figure 1). LPcm receives input primarily from SC and pretectum (Takahashi, 1985; Mason & Groos, 1981; Shi & Davis, 2001) and sends projections mostly to temporal association cortex and postrhinal cortex (Nakamura et al., 2015; Shi & Davis, 2001), whereas LPl and LPrm are well connected with visual cortex (Takahashi, 1985; Nakamura, 2015; Masterson, 2009; Bourassa & Deschenes, 1995). However, while some projections, such as retrosplenial cortex and amygdala projections from rostral LP have been studied in detail (Kamishina, et al., 2009), a quantitative analysis of rat pulvinar connectivity with visual cortex has not yet been made. The pulvinar is known to send projections broadly to visual cortex in several other species (Zhou, Maire, et al., 2017), including mice (Tohmi et al., 2014; Bennett et al., 2019), gray squirrels (Robson and Hall, 1977), carnivores (Hutchins & Updyke, 1989; Mason, 1978) and primates (Benevento & Rezak, 1976; Asanuma et al., 1985; Adams et al., 2000). Nevertheless, it is difficult to interpret the role of the pulvinar on cortical activity without a more precise understanding of the relative weights of these connections, as well as the details of where in the pulvinar these projections originate.

Of particular interest to us was whether pulvinar in rats projects more to V1 or V2. In rodents, V1 is homologous to primate V1, whereas higher visual cortex is called V2 and is subdivided into areas receiving retinotopically organized input from V1, including medial areas anteromedial (AM) and posteromedial (PM), as well as lateral areas anterolateral (AL) and lateromedial (LM) (Olavarria and Montero, 1984; Glickfeld, et al., 2014). Each of these areas likely receives some LP input, as has been demonstrated in mouse (Tohmi et al., 2014; Juavinett et al., 2019), and to AL and LM in rat (Olavarria and Torrealba, 1978; Olivarria, 1979), but it remains unclear how contributions from pulvinar differ between higher visual cortex and V1. After lesions in mouse SC, higher visual cortex optimal speed declines to match that of V1, suggesting that only higher visual cortex is affected by pulvinar (Tohmi et al., 2014). Yet mouse LP axon terminals do confer information to V1, as demonstrated by Roth et al. (2015), although it is unclear from how many LP cells these axons originate. To better understand the contributions of the pulvinar to visual cortical cells, a more complete map of its connectivity is needed.

To address these issues, we made injections of g-deleted rabies virus in V1 and higher visual cortex, as well as in lateral and rostromedial subdivisions of LP, to retrogradely label projection neurons. In this way we are able to determine whether or not there are quantitative differences in the thalamocortical and corticothalamic projections between V1 and higher visual cortex with the rat pulvinar.

Methods

Injections of modified rabies virus were carried out in nine adult female Long-Evans rats (RRID:RGD_2308852) in order to retrogradely label connected cells (Foik et al., 2018). All procedures were approved by the University of California, Irvine Institutional Animal Care and Use Committee and the Institutional Biosafety Committee, and followed the guidelines of the National Institutes of Health.

G-deleted rabies viruses (RV; Wickersham et al., 2007) modified with either green fluorescent protein (GFP) or mCherry transgenes (provided by the Callaway laboratory) were amplified and purified as described by Osakada & Callaway (2013). For each virus, BHK cells (RRID:CVCL_1915) expressing rabies glycoprotein SADB19G (RRID:Addgene_32633; B7GG, provided by the Callaway laboratory) were infected with 1 μl of stock virus and maintained at 3% CO_2 and 35°C for 5–6 d in order to produce viral supernatant (Figure 2a and 2b). The supernatants for each virus were subsequently used to infect five 150 mm dishes of the same cell line in order to amplify the viruses. Supernatants were collected twice during incubation at 3% CO_2 and 35°C after 6 and 10 days, then passed through a 0.45 μm polyethersulfone filter, and transferred to an ultracentrifuge (rotor SW28, Beckman Coulter) for 2 h at 19,400 g and 4°C. Purified virus was re-suspended in phosphate buffered saline (PBS) for 1 h at 4°C before 2% fetal bovine serum was added. Aliquots for injection were stored at −80°C. Titer was assessed by infecting HEK 293T cells (Sigma-Aldrich) with serial dilutions of modified virus, to ensure at least ~1×10^9 infectious units / mL was achieved. Figure 2 shows infected B7GG cells prior to amplification and infected 293T cells during titration.

Prior to surgery, rats were initially anesthetized with 2% isoflurane in a mixture of 30% oxygen and 70% nitrous oxide, and maintained with 1 to 1.5% isoflurane in the same mixture. Using a stereotaxic apparatus, a craniotomy was performed to expose the caudal neocortex of one hemisphere. A glass micropipette was cut to approximately 20 μm in diameter, filled with rabies virus suspension, and lowered into the brain using a motorized microdrive to a depth of roughly 800 μm for cortical injections or 4,250 μm for LP injections. Stereotaxic coordinates were used to target each structure: for V1 injections, between −6 and −8 mm from bregma and between 3.75 and 4.25 mm from the midline; for medial V2 injections, −5.5 to −6.5 mm from bregma, 2.25 mm lateral; for lateral V2 injections, −6 to −7 mm from bregma, 5.5 mm lateral; for LPrm injections, −3.75 to −4 from bregma, 1.75 mm lateral; for LPl injections, −3.75 to −4 from bregma, 2.75 mm lateral. Viral suspensions were injected at a rate of approximately 1 μl/min using an adjustable regulator and pressures below 35 kPa, to a volume of no more than 1.2 μl per injection, as larger injection volumes can cause damage to surrounding tissue. To increase total injection volume, multiple injections were made at nearby depths or nearby sites within the target area in most cases. Total injection volumes, summed across all depths and all sites for each case, are listed in Table 1 (M = 3.1 μl, SD = 1.1 μl, n = 16). Following injections, the skull was sealed with dental cement before closing the scalp with surgical staples and reviving the rat.

Following a 7–14 day survival period, rats were deeply anesthetized with Euthasol and transcardially perfused first with saline, then with 4% paraformaldehyde in PBS. Brains were removed and cryoprotected in 30% sucrose for at least 24 hours, then sectioned coronally on a freezing microtome to 40 μm thickness, mounted on glass microscope slides, and cover slipped using polyvinyl alcohol mounting medium with 1,4diazabicyclo-octane (PVA-DABCO, prepared in-house). To aid identification of areas and nuclei, sections were stained with 4,6-diamidino-2-phenylidole (DAPI; RRID:AB_2307445) prior to mounting, and cover-slipped wet to maximize myelin autofluorescence.

To assess corticothalamic connectivity, every fourth section was scanned using a fluorescent microscope (Axioplan 2, Zeiss, White Plains, NY) equipped with a 10x objective and motorized stage. Images were captured with a monochromatic low-noise CCD camera (Sensicam qe, PCO AG, Kelheim, Germany) and corrected for lamp misalignment by dividing each pixel by corresponding pixels in a flat field image acquired for each color channel. Corrected images were stitched using stage coordinates with regions of 10 overlapping pixels between images in which average pixel values were used. False colors were applied to each image before each brain section was counted manually for labeled cells. Neurons were identified based on the presence of the cell soma and dendrites. Fluorescently labeled neurons were then annotated by anatomical brain region based on myelin autofluorescence and DAPI (RRID:AB_2307445) stains in reference to the rat brain atlas by Paxinos and Watson (2013). Injection sites were identified in histology by tracks left by the glass micropipette (see Figure 3b). Image correction and stitching were performed in MATLAB (Mathworks, Natick, MA) using the multisection-imager toolbox (http://github.com/leoscholl/multisection-imager).

Statistical significance was determined based on uncorrected cell counts. P values lower than 0.05 were considered significant for Student's *t*-tests and two-way ANOVAs. All statistical analyses were carried out in MATLAB.

Results

To assess the strength and size of input from LP to V1, we made four injections of the retrograde fluorescent-protein-expressing g-deleted rabies virus into V1 of two rats. In each case, substantial thalamic labeling was observed when calculated as a percentage of the total number of labeled neurons in each case ($M = 11\%$, $SD = 6\%$, n = 4).

In rat R1703, one large injection was made in anterior V1 (GFP; Figure 4a), and a second in posterior V1 (mCherry; Figure 4a). The resulting fluorescent labeling included a large number of cortical cells in and around the injection sites. In the thalamus, 30 labeled cells were found in LGN and only seven in LP across the two injections (see Table 2). Topographic organization of LGN labeling was observed between the two injection sites, with the posterior V1 injection labeling anterior LGN and vice versa, consistent with previous findings in the rat (Sauve & Gaillard, 2007). No such topography was seen for LP cells in this case, presumably because there were too few labeled cells; retinotopy has been reported in mice (Roth et al., 2015; Juavinett et al., 2019).

In rat R1802, three small injections were made spanning anterior to posterior V1 for each virus (Figure 4b), in order to infect a large area of V1 axon terminals while keeping the total injection volume comparable to the previous injections. Labeled cells in LGN were spread along the anterior posterior axis in both cases. Since the injections of each virus were paired locally, topography was not analyzed in this rat. In total, 49 cells were labeled in LGN and 11 in LP across the six injections (see Table 2). Cells were found in all three LP subdivisions in both cases.

Across the four cases with V1 injections (see Table 2), there were significantly fewer inputs from LP to V1 compared to the number of inputs from LGN to V1 ($p = 0.01$, paired samples *t*-test). Infecting a large area of V1 on the possibility that LP input to V1 is sparse made no difference; there was one fifth as many cells in LP as in LGN in both R1703 and R1802.

In contrast to V1, injections in V2 labeled proportionately fewer neurons in LGN and many more neurons in LP. In rat R1902, the anterior and posterior medial V2 areas, AM and PM, were each injected with rabies virus (Figure 5a). The resulting fluorescence in the thalamus was primarily located within LP, 179 cells, compared to the LGN, 6 cells, indicating the injections were well contained outside V1. Between LP subdivisions, only four cells were labeled in LPcm, while 95 were labeled in LPl and 80 in LPrm (see Table 2 for summary). The cells in LPl and LPrm were not distributed throughout each subdivision, rather they were clustered along the medial margin of LPl and central LPrm (see Figure 5a).

Lateral V2 areas AL and LM were targeted with single injections into rats R1630 and R1803, respectively. These injections were three times smaller than the injections in R1902, yet thalamic labeling was also limited primarily to the LP in these cases, as 26 neurons were located in LP and 7 in the LGN. Between LP subdivisions, LPl had the majority of fluorescent cells in both cases, with 73% of LP cells being found within LPl in R1630 and 80% in R1803 (see Table 2).

Across all four cases with V2 injections, there was a significantly higher percentage of cells labeled in LP than in LGN ($p < 0.01$, paired samples *t*-test; see Table 2). Moreover, compared with V1 injections, V2 injections revealed that LP sends significantly more projections to V2 than it does to V1. The number of labeled cells in LP following V2 virus injections was significantly larger than the number following V1 injections ($F(1,12) = 6.1$, $p = 0.03$, *ANOVA*). Additionally, medial V2 areas AM and PM were both observed to receive more LP input than lateral V2 areas AL and LM, especially from LPrm. There was also some indication that lateral V2 areas receive less input from LPrm (n.s.), however there was no difference between overall input to V2 between LPrm and LPl ($F(1,12) = 0.28$, $p = 0.6$, *ANOVA*).

Injections of modified rabies virus were also made into LPrm and LPl to retrogradely determine the strength of corticothalamic inputs from V1 and V2 to each pulvinar subdivision. Figure 6 illustrates three cases with injections targeting similar stereotaxic coordinates for LPrm and LPl. Rats R1903 (Figure 6a) and R1909 (Figure 6c) had large injections targeting central LPl and LPrm; rat R1909 (Figure 6b) had large injections targeting central LPl but more posterior LPrm. In these three rats, fluorescent labeling was observed in the SC following both LPrm and LPl injections, indicating some overlap between injection sites or spread into the tecto-recipient LPcm. Rat R1905 (Figure 7) had small injections into anterior LPl and LPrm (see Table 1); very few SC cells were labeled following LPrm injection in this case, whereas many were labeled following LPl injection.

Cortical labeling was assessed in each case to determine the relative strength of inputs from V1 and V2 to each injected LP subdivision. In all cases, V2 labeling accounted for most of the cortical fluorescence (~75%; Table 3). Consistent labeling was also seen in

somatosensory, auditory, and association cortex following injections into LPrm and LPl. Rat R1903 additionally had significant reticular thalamic nucleus labeling following injection into LPl (Figure 6a), which is known to project to the pulvinar and many other neighboring thalamic nuclei (Lyon et al., 2010; Bourassa & Deschenes, 1995; Zikopoulos & Barbas, 2007; Hirsch et al., 2015). Also of note, rat R1909 had significant amygdala labeling following injection into LPrm, but this is perhaps due to leakage of virus into the hippocampus directly dorsal to LP.

A significantly higher number of cells were labeled in V2 areas than in V1 ($F(1,12) = 5.39$, $p = 0.04$, *ANOVA*). Furthermore, injections in LPl led to significantly more labeling in visual cortex than injections in LPrm ($F(1,12) = 5.35$, $p = 0.04$, *ANOVA*), implying that rat pulvinar receives differential visual cortical inputs along its medial-lateral axis. V1 and V2 cells were located in layers 5 and 6. The percentage of visual cortex cells in each layer for each case is listed in Table 3. On average, more cells were labeled in layer 6 than in layer 5 in both V1 (M = 70% layer 6, SD = 27%) and V2 (M = 77% layer 6, SD = 17%).

Discussion

The purpose of this study was to compare the connections of V1 and higher visual cortex with the pulvinar as well as to determine any anatomical differences between lateral and medial pulvinar subdivisions in the rat. We demonstrated that the projections in both directions between pulvinar and V2 in rats are more frequent than those between pulvinar and V1, suggesting that the pulvinar has a greater influence on activity in higher visual cortex than in V1. We also observed differences in the number of inputs and outputs of LP subdivisions, with the lateral portion of the pulvinar having a stronger connection to visual cortex, for both V2 and V1. Together, these results provide a basis for understanding to which visual networks the rat pulvinar contributes.

While our conclusions rest on the assumption that there is an absence of selectivity of infection by rabies virus, in previous studies of the pulvinar, projections have been identified to both V1 and higher visual cortices in a manner consistent with our findings. In rats, anterograde injections in LP labeled both V1 and V2, but V1 labeling was much more sparse, with many more fibers being labeled in both medial and lateral V2 (Nakamura et al., 2015, see their Figure 7). In mice, retrograde injections in V1 produced fluorescent labeling that was confined to small regions within LP, whereas injections in other visual cortical areas led to larger and brighter patches of fluorescent labeling (Juavinett et al., 2019, see their Figure 4). Although qualitative, these previous findings are consistent with the difference in projection strength we observed in the present study.

In other species, there is also a trend in the existing literature of denser and more numerous projections from pulvinar to higher visual cortex compared to projections from pulvinar to V1. In squirrels, a highly visual rodent, dense pulvinar labeling was observed following retrograde tracer injections into the temporal posterior area and visual area 19, but very few cells were labeled following V1 (area 17) injection (Robson & Hall, 1977, see their Figures 15–17). Tree shrew, a close primate relative, exhibits a similar pattern of connectivity following retrograde tracer injections in V1 and V2; only sparse, topographic labeling was

observed in caudal pulvinar following V1 injection, whereas V2 injection was followed by denser labeling spread across large regions of caudal and ventral pulvinar (Lyon et al., 2003, see their Figure 2). In galagos, a prosimian primate, up to two times as many neurons were labeled in V2 than V1 by pulvinar retrograde tracer injections (Moore et al. 2019). In macaque monkeys, Lysakowski et al. (1988) observed about twice as many V2 projections from pulvinar compared to V1 projections (see their Figure 2). Similarly, Kennedy & Bullier (1985) counted cells following V1 and V2 injections in macaque; 7–35% of labeled cells in the lateral pulvinar were from V1 versus 50–70% from V2 (their Figure 16 or Table VI).

This view is also consistent with the results of Tohmi et al. (2014), who showed higher visual areas in mice behave more like V1 when the extrageniculate pathway is damaged by SC lesions. Our results suggest the tecto-recipient LPl has the circuitry to drive these changes to higher visual cortex responses. In addition, Zhou et al. (2016) found that deactivation of the ventrolateral pulvinar in monkeys led to inactivity in V4, without evidence for change in V1 activity, implying a direct influence of pulvinar on higher visual cortex. Nevertheless, pulvinar does also project to V1 and can have significant functional effects on neurons there (Purushothaman et al., 2012). Our results that V2 receives the bulk of the pulvinar input, around 75% (Table 3), compared to V1, also draws comparsions to the core versus matrix distinction of the thalamus (Jones, 1998), where V1 receives the less driving matrix input from pulvinar and V2 receives driving core and matrix input. Along these lines, Nakamura et al. (2015) showed that rat LP projects primarily to layer 1 in V1, signaling a modulatory matrix-like input, and predominantly to layers 4 and 5 in V2, indicating a core-type input. Similar results have been reported in monkeys (see Rockland et al. 2019).

In primates, the pulvinar is divided by its connectivity with cortical areas into a dorsalventral stream classification for visually guided actions and object vision, respectively. The posterior and caudomedial inferior pulvinar (PIp and PIcm) as well as the medial inferior pulvinar (PIm) are associated with the dorsal stream because they receive inputs from SC and project to dorsal stream areas such as the middle temporal visual area (MT), whereas the caudolateral inferior (PIcl) portion and lateral (PL) portions of the pulvinar are associated with the ventral stream because of their projections to early visual areas and inferior temporal cortex (Kaas and Lyon, 2007; for alternative primate pulvinar nomenclature see Gutierrez et al. 1995). As illustrated in Figure 8, SC and visual cortex input to pulvinar is highly conserved across species, with regions of dense bilateral input from SC, ipsilateral input from SC, and cortical input only. These include rat (Takahashi, 1985; Mason & Groos, 1980), mouse (Zhou, Maire, et al., 2017), gray squirrel (Baldwin et al., 2011), tree shrew (Lyon et al., 2003), and primate (Baldwin et al., 2013). Given that they share anatomical features with primates, rodents might be a suitable model animal for studying pulvinar contributions to the two visual streams, as there is growing evidence for such a classification in rodents (Wang et al., 2011; Glickfeld, 2014; Nishio et al., 2018). In the most basic sense the pathway relaying visual information from SC through LPcm to cortex in rodent could be linked to the dorsal stream; whereas the LPrm subdivision which does not relay SC inputs could be linked to the ventral stream (Schneider, 1969; Lyon et al., 2010).

Finally, the data presented here suggest that pulvinar subdivisions are involved in both top-down and bottom-up forms of visual processing. In monkeys, disruption of the dorsolateral pulvinar has been shown to cause deficits to spatial attention (Wilke et al., 2010), however it is unclear whether the pulvinar directs feedforward salience-based selection, top-down attention, or both. If the pulvinar were to encode a salience map, it would likely send this information directly to V1 where bottom-up salience information begins in the cortex (Zhang et al., 2012). However, we confirmed in rats the prevalence of higher visual cortex connections with the pulvinar, and the relatively weaker connection between V1 and the pulvinar, implying that salience cannot be the only function carried out by any pulvinar subdivision. Instead, additional top-down modulation of features such as motion or texture in higher visual cortex (Schiller, 1993; Saalmann et al., 2012; Perry & Fallah, 2014) might be directed by the pulvinar under attentional demands, either via subcortical input from the thalamic reticular nucleus or brainstem (FitzGibbon, 1994; Fitzpatrick, et al., 1989) or from attention signals in the cortex (Zhou et al., 2016).

Acknowledgements

This work was supported by the Whitehall Foundation #2014-08100 (DCL) and the National Eye Institute R01EY024890 (DCL).

References

Adams MM, Hof PR, Gattass R, Webster MJ, & Ungerleider LG (2000). Visual cortical projections and chemoarchitecture of macaque monkey pulvinar. Journal of Comparative Neurology, 419(3), 377–393. 10.1002/(SICI)10969861(20000410)419:3<377::AID-CNE9>3.0.CO;2-E

Asanuma C, Andersen RA, & Cowan WM (1985). The thalamic relations of the caudal inferior parietal lobule and the lateral prefrontal cortex in monkeys: Divergent cortical projections from cell clusters in the medial pulvinar nucleus. Journal of Comparative Neurology, 241(3), 357–381. 10.1002/cne.902410309

Baldwin MKL, Balaram P, & Kaas JH (2013). Projections of the superior colliculus to the pulvinar in prosimian galagos (Otolemur garnettii) and VGLUT2 staining of the visual pulvinar. Journal of Comparative Neurology, 521(7), 1664–1682. 10.1002/cne.23252

Baldwin MKL, Wong P, Reed JL, & Kaas JH (2011). Superior colliculus connections with visual thalamus in gray squirrels (Sciurus carolinensis): Evidence for four subdivisions within the pulvinar complex. Journal of Comparative Neurology, 519(6), 1071–1094. 10.1002/cne.22552

Bender DB (1982). Receptive-field properties of neurons in the macaque inferior pulvinar. Journal of Neurophysiology, 48(1), 1–17. 10.1152/jn.1982.48.1.1 [PubMed: 7119838]

Benevento L. a., & Rezak M (1976). The cortical projections of the inferior pulvinar and adjacent lateral pulvinar in the rhesus monkey (Macaca mulatta): an autoradiographic study. Brain Research, 108(1), 1–24. 10.1016/00068993(76)90160-8 [PubMed: 819095]

Bennett C, Gale SD, Garrett ME, Newton ML, Callaway EM, Murphy GJ, & Olsen SR (2019). Higher-Order Thalamic Circuits Channel Parallel Streams of Visual Information in Mice. Neuron, 1–16. 10.1016/j.neuron.2019.02.010

Bourassa J, & Deschenes M (1995). Corticothalamic projections from the primary visual cortex in rats: a single fiber study using biocytin as an anterograde tracer. Neuroscience, 66(2), 253–263. 10.1016/0306-4522(95)00009-8 [PubMed: 7477870]

Espinoza SG, & Thomas HC (1983). Retinotopic organization of striate and extrastriate visual cortex in the hooded rat. Brain Research, 272(1), 137–144. 10.1016/0006-8993(83)90370-0 [PubMed: 6616189]

FitzGibbon T (1994). Rostral Reticular Nucleus of the Thalamus Sends a Patchy Projection to the Pulvinar Lateralis-Posterior Complex of the Cat. Experimental Neurology, 129(2), 266–278. 10.1006/exnr.1994.1169 [PubMed: 7525333]

Fitzpatrick D, Diamond IT, & Raczkowski D (1989). Cholinergic and monoaminergic innervation of the cat's thalamus: Comparison of the lateral geniculate nucleus with other principal sensory nuclei. Journal of Comparative Neurology. 10.1002/cne.902880411

Foik AT, Scholl LR, Lean GA, Aramant RB, McLelland BT, Seiler MJ, … Lyon DC (2018). Detailed Visual Cortical Responses Generated by Retinal Sheet Transplants in Rats with Severe Retinal Degeneration. The Journal of Neuroscience, 38(50), 10709–10724. 10.1523/jneurosci.1279-18.2018 [PubMed: 30396913]

Glickfeld LL, Reid RC, & Andermann ML (2014). A mouse model of higher visual cortical function. Current Opinion in Neurobiology, 24(1), 28–33. 10.1016/j.conb.2013.08.009 [PubMed: 24492075]

Goodale MA (2005). Action insight: The role of the dorsal stream in the perception of grasping. Neuron. 10.1016/j.neuron.2005.07.010

Goodale MA (2013). Separate visual systems for perception and action: a framework for understanding cortical visual impairment. Developmental Medicine & Child Neurology. 10.1111/dmcn.12299

Gutierrez C, Yaun A, Cusick CG (1995) Neurochemical subdivisions of the inferior pulvinar in macaque monkeys. Journal of Comparative Neurology. 363(4):545–562. DOI: 10.1002/cne.903630404

Hirsch JA, Wang X, Sommer FT, & Martinez LM (2015). How Inhibitory Circuits in the Thalamus Serve Vision. Annual Review of Neuroscience, 38(1), 309–329. 10.1146/annurev-neuro-071013-014229

Hutchins B, & Updyke BV (1989). Retinotopic organization within the lateral posterior complex of the cat. Journal of Comparative Neurology, 285(3), 350–398. 10.1002/cne.902850306

Jaramillo J, Mejias JF, & Wang XJ (2019). Engagement of Pulvino-cortical Feedforward and Feedback Pathways in Cognitive Computations. Neuron, 101(2), 321–336.e9. 10.1016/j.neuron.2018.11.023 [PubMed: 30553546]

Jones EG (1985). Thalamus. Plenum. 10.1007/978-1-4615-1749-8

Jones EG (1998). Viewpoint: the core and matrix of thalamic organization. Neuroscience. 1998 7;85(2):331–45. DOI: 10.1016/s0306-4522(97)00581-2 [PubMed: 9622234]

Juavinett AL, Kim EJ, Collins HC, & Callaway EM (2019). A systematic topographical relationship between mouse lateral posterior thalamic neurons and their visual cortical projection targets. Journal of Comparative Neurology, (7), cne.24737. 10.1002/cne.24737

Kaas JH & Huerta MF (1988) Subcortical visual system of primates In: Steklis HP, editor. Comparative Primate Biology. New York: Alan R. Liss p 327–391.

Kaas JH, & Lyon DC (2007). Pulvinar contributions to the dorsal and ventral streams of visual processing in primates. Brain Research Reviews, 55(2 SPEC. ISS), 285–296. 10.1016/j.brainresrev.2007.02.008 [PubMed: 17433837]

Kamishina H, Conte WL, Patel SS, Tai RJ, Corwin JV, & Reep RL (2009). Cortical connections of the rat lateral posterior thalamic nucleus. Brain Research, 1264, 39–56. 10.1016/j.brainres.2009.01.024 [PubMed: 19368845]

Kennedy H, & Bullier J (1985). A double-labeling investigation of the afferent connectivity to cortical areas V1 and V2 of the macaque monkey. Journal of Neuroscience, 5(10), 2815–2830. 10.1523/jneurosci.05-10-02815.1985 [PubMed: 3840201]

Lyon DC, Jain N, & Kaas JH (2003). The visual pulvinar in tree shrews II. Projections of four nuclei to areas of visual cortex. The Journal of Comparative Neurology, 467(4), 607–627. 10.1002/cne.10940 [PubMed: 14624492]

Lyon DC, Nassi JJ, & Callaway EM (2010). A Disynaptic Relay from Superior Colliculus to Dorsal Stream Visual Cortex in Macaque Monkey. Neuron. 10.1016/j.neuron.2010.01.003

Lysakowski A, Standage GP, & Benevento LA (1988). An investigation of collateral projections of the dorsal lateral geniculate nucleus and other subcortical structures to cortical areas V1 and V4 in the macaque monkey: A double label retrograde tracer study. Experimental Brain Research, 69(3), 457–472. 10.1007/BF00247317

Mason R (1978). Functional organization in the cat's pulvinar complex. Experimental Brain Research, 31(1), 51–66. 10.1007/BF00235804 [PubMed: 639910]

Mason R, & Groos GA (1981). Cortico-recipient and tecto-recipient visual zones in the rat's lateral posterior (pulvinar) nucleus: An anatomical study. Neuroscience Letters, 25(2), 107–112. 10.1016/0304-3940(81)90316-5 [PubMed: 6168985]

Masterson SP, Li J, & Bickford ME (2009). Synaptic organization of the tectorecipient zone of the rat lateral posterior nucleus. Journal of Comparative Neurology, 515(6), 647–663. 10.1002/cne.22077

Mizzi R, & Michael G. a. (2014). The role of the collicular pathway in the salience-based progression of visual attention. Behavioural Brain Research, 270, 330–338. 10.1016/j.bbr.2014.05.043 [PubMed: 24880095]

Nakamura H, Hioki H, Furuta T, & Kaneko T (2015). Different cortical projections from three subdivisions of the rat lateral posterior thalamic nucleus: A single-neuron tracing study with viral vectors. European Journal of Neuroscience, 41(10), 1294–1310. 10.1111/ejn.12882

Nishio N, Tsukano H, Hishida R, Abe M, Nakai J, Kawamura M, … Shibuki K (2018). Higher visual responses in the temporal cortex of mice. Scientific Reports, 8(1), 1–12. 10.1038/s41598-018-29530-3 [PubMed: 29311619]

Olavarria J (1979). A horseradish peroxidase study of the projections from the lateroposterior nucleus to three lateral peristriate areas in the rat. Brain Res. 1979 9 7;173(1):137–41. DOI: 10.1016/0006-8993(79)91101-6 [PubMed: 487075]

Olavarria J, & Torrealba F (1978). The effect of accute lesions of the striate cortex on the retinotopic organization of the lateral peristriate cortex in the rat. Brain Res. 1978 8 4;151(2):386–91. DOI: 10.1016/0006-8993(78)90894-6 [PubMed: 679016]

Olavarria J, & Montero VM (1984). Relation of callosal and striate-extrastriate cortical connections in the rat: Morphological definition of extrastriate visual areas. Experimental Brain Research, 54(2), 240–252. 10.1007/BF00236223 [PubMed: 6723844]

Osakada F, & Callaway E (2013). Design and generation of recombinant rabies virus vectors. Nature Protocols, 8(8), 1583–1601. 10.1038/nprot.2013.094 [PubMed: 23887178]

Paxinos G, Watson C (2013). The Rat Brain in Stereotaxic Coordinates (7th ed.). London: Academic Press.

Perry CJ, & Fallah M (2014). Feature integration and object representations along the dorsal stream visual hierarchy. Frontiers in Computational Neuroscience, 8(8), 1–17. 10.3389/fncom.2014.00084 [PubMed: 24550816]

Petersen SE, Robinson DL, & Keys W (1985). Pulvinar nuclei of the behaving rhesus monkey: Visual responses and their modulation. Journal of Neurophysiology, 54(4), 867–886. 10.1152/jn.1985.54.4.867 [PubMed: 4067625]

Purushothaman G, Marion R, Li K, & Casagrande V. a. (2012). Gating and control of primary visual cortex by pulvinar. Nature Neuroscience, 15(6), 905–912. 10.1038/nn.3106 [PubMed: 22561455]

Robinson DL, Petersen SE, & Keys W (1986). Saccade-related and visual activities in the pulvinar nuclei of the behaving rhesus monkey. Experimental Brain Research. Experimentelle Hirnforschung. Experimentation Cerebrale, 62(3), 625–634. 10.1007/BF00236042 [PubMed: 3720891]

Robson JA, & Hall WC (1977). The organization of the pulvinar in the grey squirrel (Sciurus carolinensis). I. Cytoarchitecture and connections. Journal of Comparative Neurology, 173(2), 355–388. 10.1002/cne.901730210

Rockland KS (2019). Distinctive spatial and laminar organization of single axons from lateral pulvinar in the macaque. Vision (Basel). 4(1). pii: E1. doi: 10.3390/vision4010001.

Roth MM, Dahmen JC, Muir DR, Imhof F, Martini FJ, & Hofer SB (2015). Thalamic nuclei convey diverse contextual information to layer 1 of visual cortex. Nature Neuroscience, 19(2), 299–307. 10.1038/nn.4197 [PubMed: 26691828]

Saalmann YB, Pinsk M. a., Wang L, Li X, & Kastner S (2012). The Pulvinar Regulates Information Transmission Between Cortical Areas Based on Attention Demands. Science, 337(6095), 753–756. 10.1126/science.1223082 [PubMed: 22879517]

Sauve Y, Gaillard F Regeneration in the Visual System of Adult Mammals (2005). In: Kolb H, Fernandez E, Nelson R, editors. Webvision: The Organization of the Retina and Visual System. Salt Lake City (UT): University of Utah Health Sciences Center; 1995-.

Schiller PH (1993). The effects of V4 and middle temporal (MT) area lesions on visual performance in the rhesus monkey. Visual Neuroscience. 10:717–746. 10.1017/S0952523800005423 [PubMed: 8338809]

Schneider GE (1969). Two visual systems. Science. 163 (3870): 895–902. doi:10.1126/science.163.3870.895. [PubMed: 5763873]

Sereno MI, & Allman JM (1991). Cortical visual areas in mammals The Neural Basis of Visual Function. p 160–172. London: Macmillan.

Shi C, & Davis M (2001). Visual Pathways Involved in Fear Conditioning Measured with Fear-Potentiated Startle: Behavioral and Anatomic Studies. The Journal of Neuroscience, 21(24), 9844–9855. 10.1523/JNEUROSCI.21-2409844.2001 [PubMed: 11739592]

Stepniewska I (2003). The pulvinar In: JH Kaas CE Collins, editors. The primate visual system. Boca Raton, FL: CRC Press p 53–80.

Takahashi T (1985). The organization of the lateral thalamus of the hooded rat. The Journal of Comparative Neurology, 231(3), 281–309. 10.1002/cne.902310302 [PubMed: 3968240]

Tohmi M, Meguro R, Tsukano H, Hishida R, & Shibuki K (2014). The extrageniculate visual pathway generates distinct response properties in the higher visual areas of mice. Current Biology : CB, 24(6), 587–597. 10.1016/j.cub.2014.01.061 [PubMed: 24583013]

Veale R, Hafed ZM, & Yoshida M (2017). How is visual salience computed in the brain? Insights from behaviour, neurobiology and modeling. Philosophical Transactions of the Royal Society B: Biological Sciences, 372(1714). 10.1098/rstb.2016.0113

Wang Q, & Burkhalter A (2007). Area map of mouse visual cortex. The Journal of Comparative Neurology, 502(3), 339–357. 10.1002/cne.21286 [PubMed: 17366604]

Wang Q, Gao E, & Burkhalter A (2011). Gateways of ventral and dorsal streams in mouse visual cortex. Journal of Neuroscience, 31(5), 1905–1918. 10.1523/JNEUROSCI.3488-10.2011 [PubMed: 21289200]

Wickersham I, Lyon D, Barnard R, & Mori T (2007). Monosynaptic restriction of transsynaptic tracing from single, genetically targeted neurons. Neuron, 53(5), 639–647. 10.1016/j.neuron.2007.01.033 [PubMed: 17329205]

Wilke M, Mueller K-M, & Leopold DA (2009). Neural activity in the visual thalamus reflects perceptual suppression. Proceedings of the National Academy of Sciences, 106(23), 9465–9470. 10.1073/pnas.0900714106

Wilke M, Turchi J, Smith K, Mishkin M, & Leopold DA (2010). Pulvinar Inactivation Disrupts Selection of Movement Plans. Journal of Neuroscience, 30(25), 8650–8659. 10.1523/JNEUROSCI.0953-10.2010 [PubMed: 20573910]

Zhang X, Zhaoping L, Zhou T, & Fang F (2012). Neural Activities in V1 Create a Bottom-Up Saliency Map. Neuron, 73(1), 183–192. 10.1016/j.neuron.2011.10.035 [PubMed: 22243756]

Zhou H, Schafer RJ, & Desimone R (2016). Pulvinar-Cortex Interactions in Vision and Attention. Neuron, 89(1), 209–220. 10.1016/j.neuron.2015.11.034 [PubMed: 26748092]

Zhou N, Masterson S, Damron J, Guido W, & Bickford M (2017). The mouse pulvinar nucleus links the lateral extrastriate cortex, striatum, and amygdala. The Journal of Neuroscience, 1279–17. 10.1523/JNEUROSCI.1279-17.2017

Zhou NA, Maire PS, Masterson SP, & Bickford ME (2017). The mouse pulvinar nucleus: Organization of the tectorecipient zones. Visual Neuroscience. 10.1017/S0952523817000050

Zikopoulos B, & Barbas H (2007). Circuits for multisensory integration and attentional modulation through the prefrontal cortex and the thalamic reticular nucleus in primates. Reviews in the Neurosciences, 18(6), 417–438. 10.1016/j.cub.2012.07.015 [PubMed: 18330211]

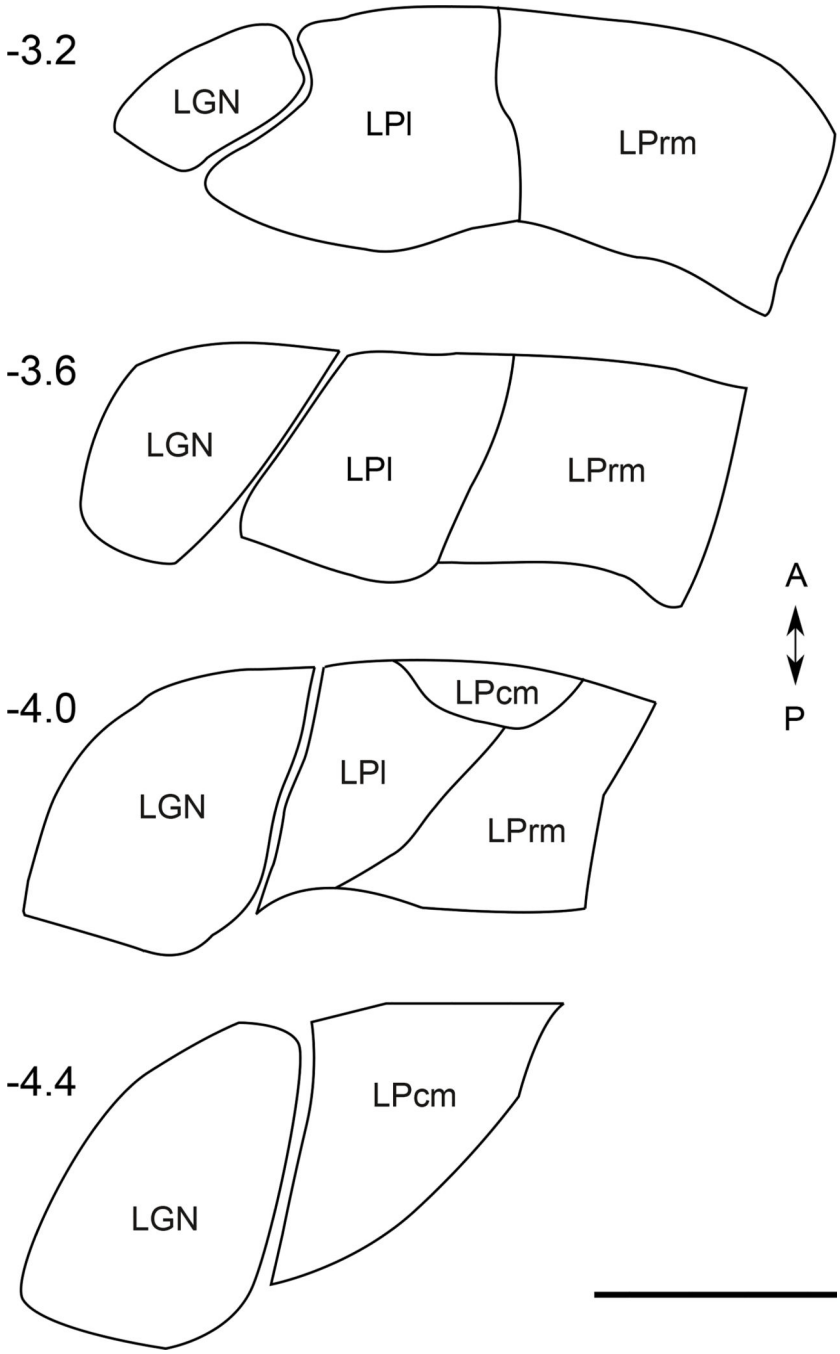

Figure 1.

Schematic of rat lateral (LPl), rostromedial (LPrm) and caudomedial (LPcm) pulvinar subdivisions and the lateral geniculate nucleus (LGN) between −3.2 and −4.4 mm from bregma. Based on the cytoarchitectonic divisions by Nakamura (2015), conformed to the atlas by Paxinos and Watson (2013).

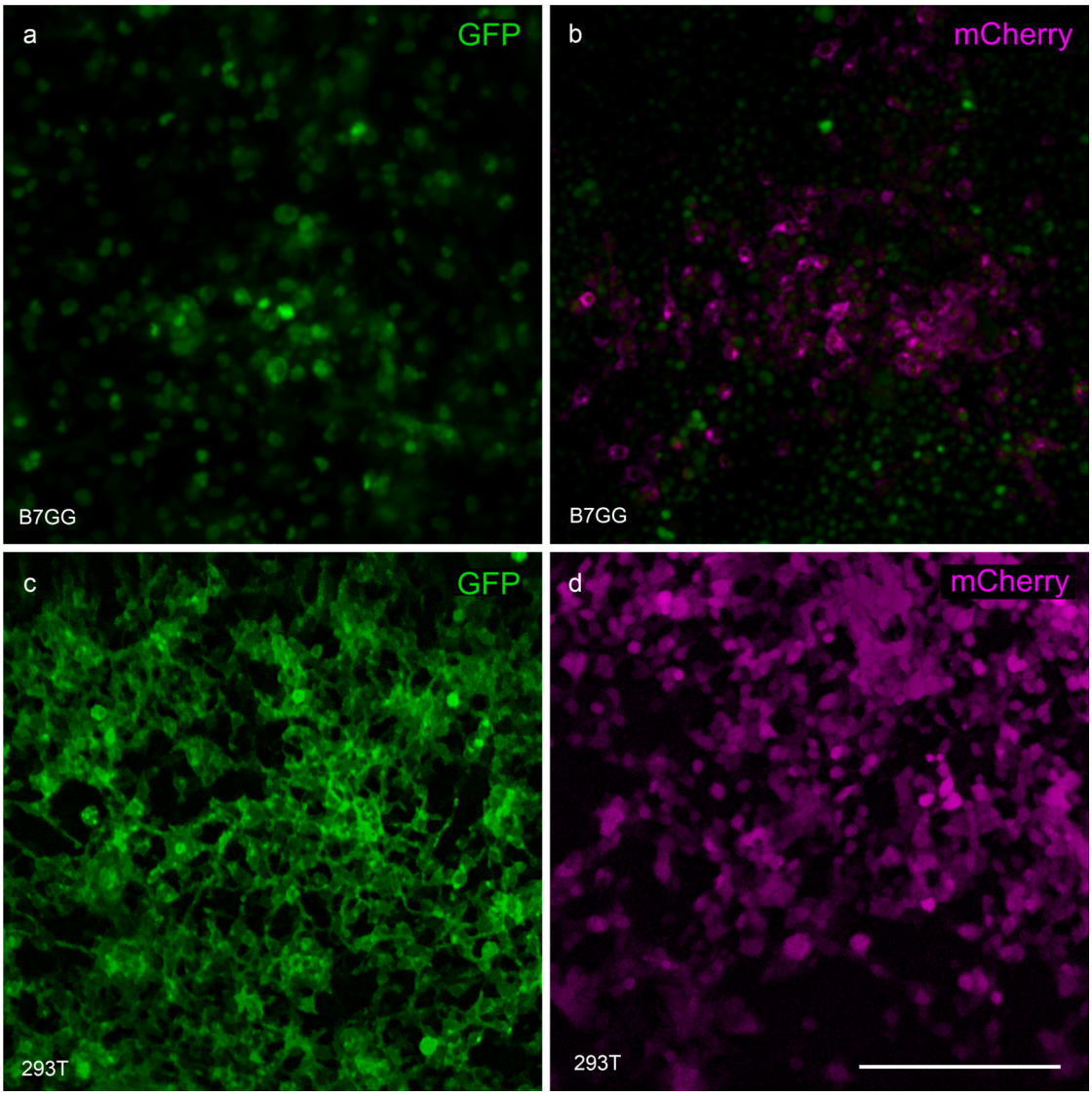

Figure 2.

Amplification and titration of GFP and mCherry modified rabies viruses. B7GG cells in (a) and (b) express nuclear GFP in addition to the rabies viruses being amplified. 293T cells shown in (c) and (d) were used to verify expression of the viruses without the presence of cellular rabies glycoprotein and to quantify the virus titers. Scale bar equals 250 μm.

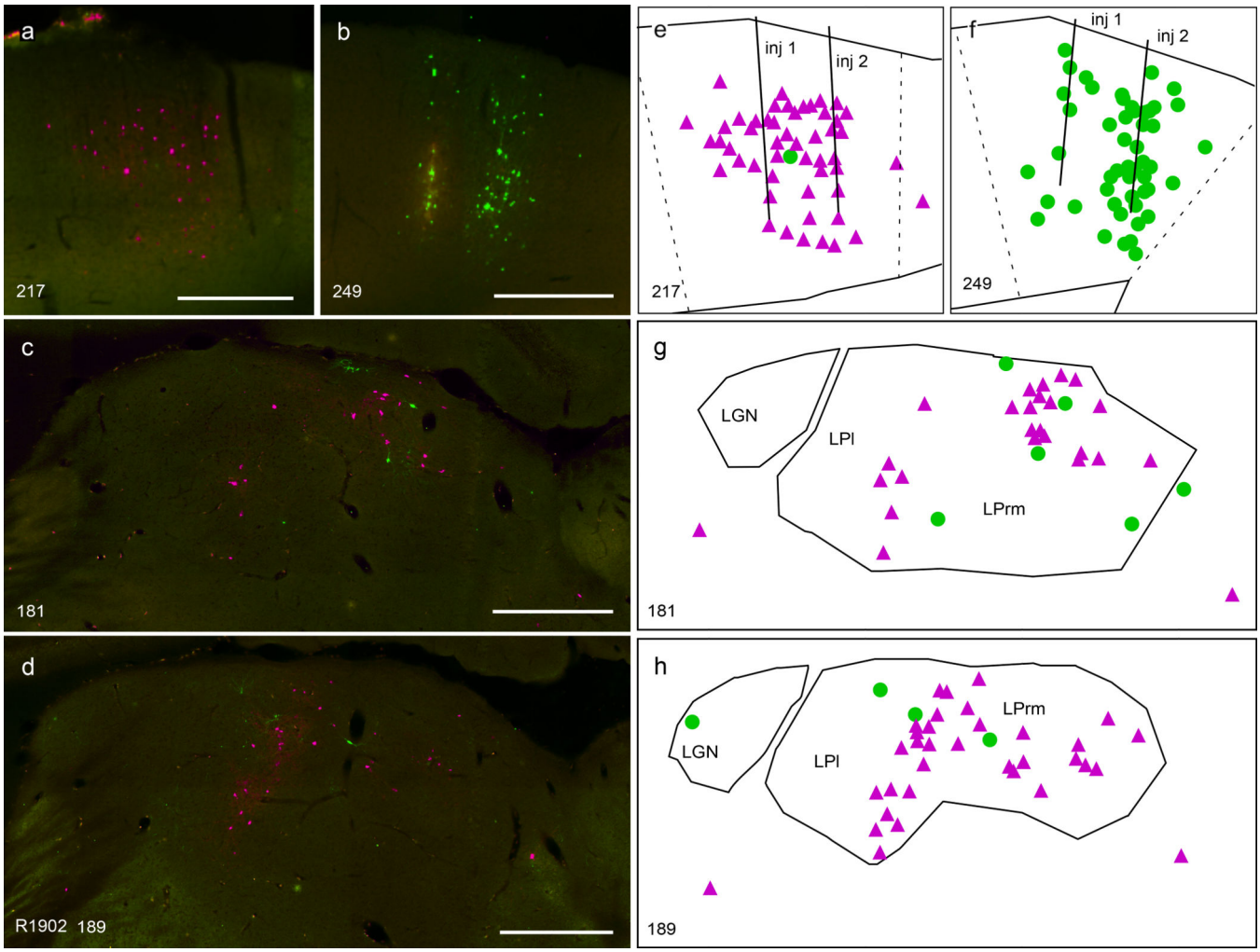

Figure 3.

Representative example showing fluorescently labeled thalamic inputs to anterior and posterior medial V2 areas AM and PM after injections of mCherry (a and e; magenta) and GFP (b and f; green) modified rabies viruses in rat R1902. Thalamic labeling (c-h) reveals a large population of LPl and LPrm projections to V2. False-color stitched fluorescent images are shown in a-d. Reconstructions of the same sections are shown in e-h. Scale bars equal 500 μm.

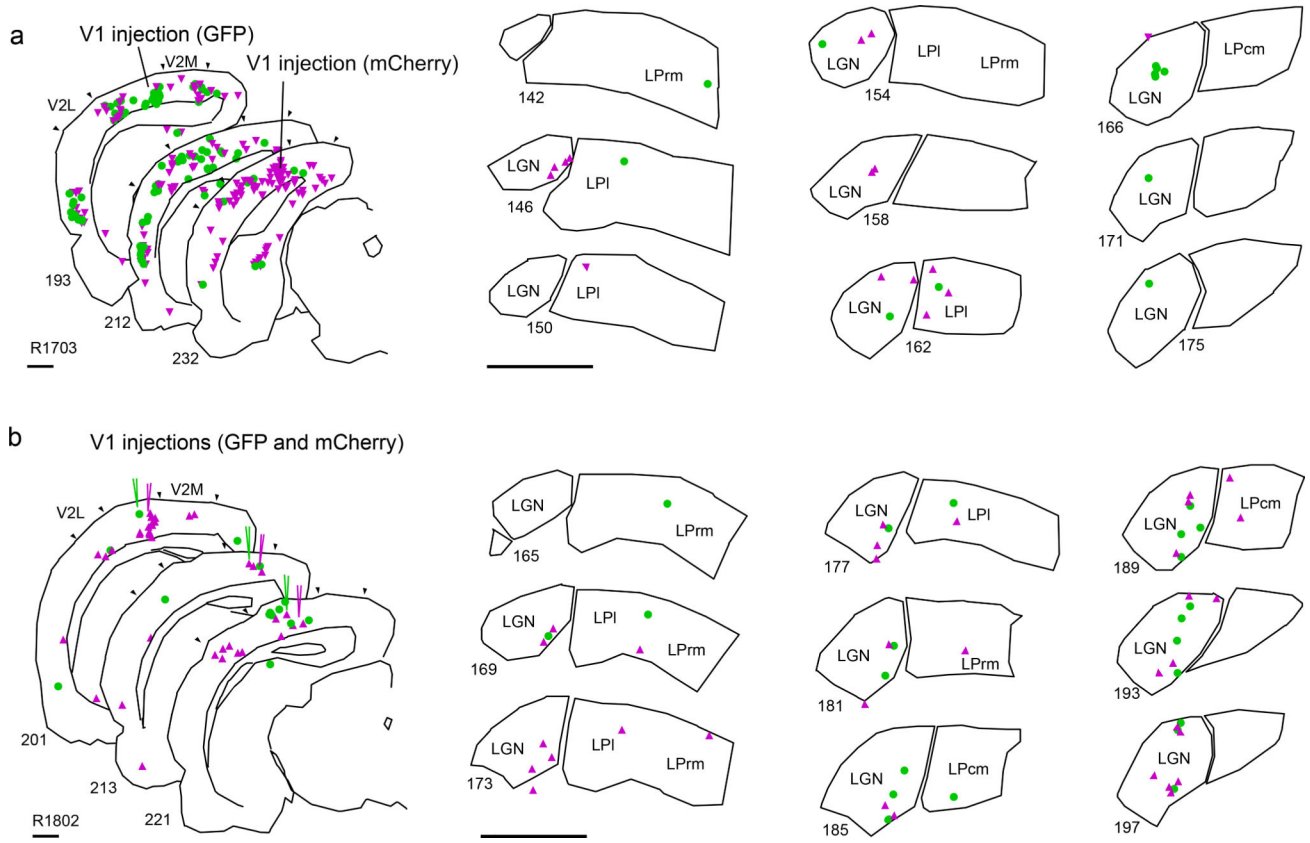

Figure 4.

Reconstructions of fluorescently labeled neurons identified after retrograde RV injections in V1. In rat R1703 (a), the GFP virus was injected into the anterior portion of V1 and the mCherry virus was injected into posterior V1. In rat R1802 (b), three smaller injections were made along the anterior-posterior axis of V1 for each virus, covering a large portion of V1. In all cases, more labeled neurons were present in LGN than in pulvinar. Magenta triangles indicate mCherry fluorescence, green circles indicate GFP. Scale bars equal 1 mm.

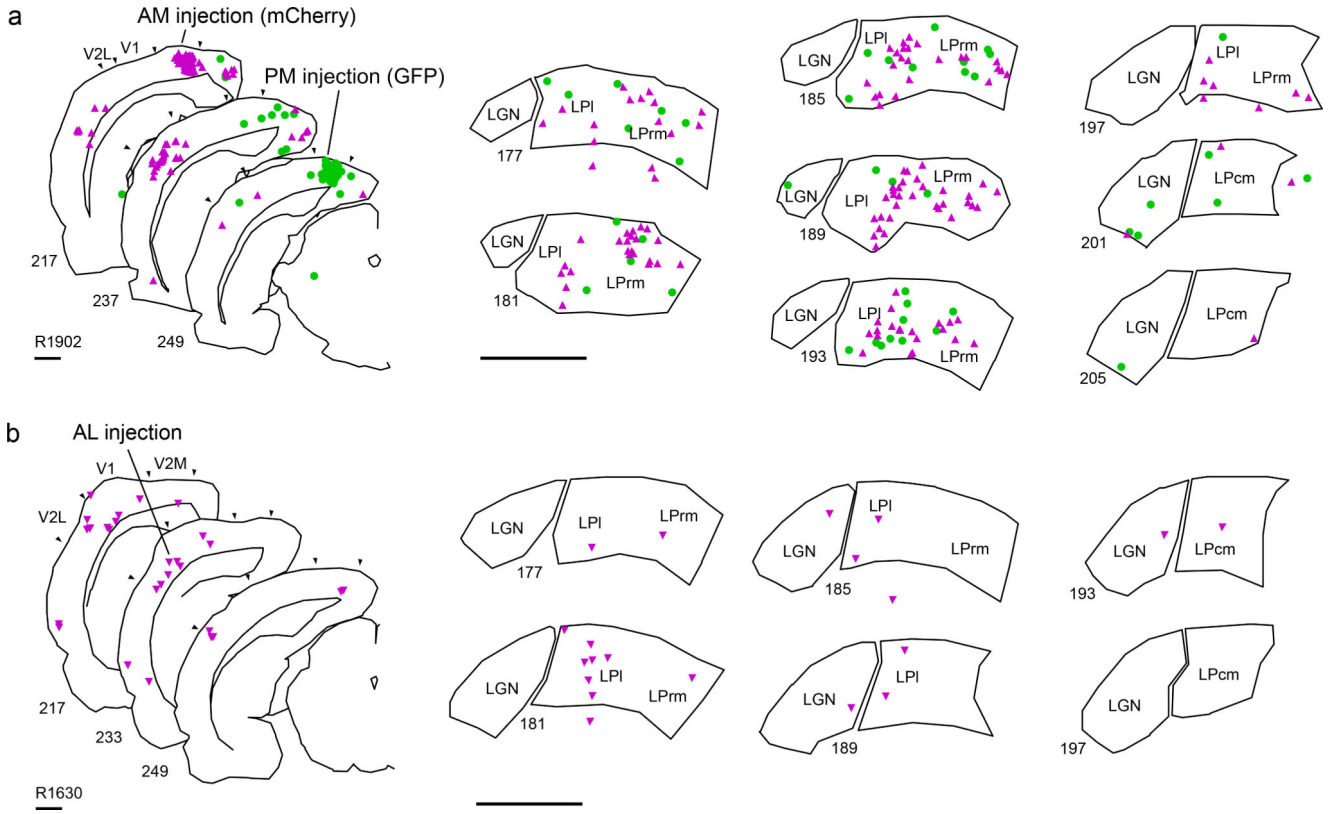

Figure 5.

Reconstructed fluorescent labeling for rats with injections in V2 areas. Rat R1902 (a) was injected with mCherry virus targeting anteromedial V2 (area AM), and GFP virus targeting the posteromedial V2 (area PM). Labeling in the thalamus was strong in both LPrm and LPl, with only a few labeled cells in the lateral geniculate nucleus (LGN). Rat R1630 (b) was injected with mCherry virus targeting anterolateral V2 (area AL), resulting in thalamic labeling mostly in LPl. Magenta triangles indicate mCherry fluorescence, green circles indicate GFP. Scale bars equal 1 mm.

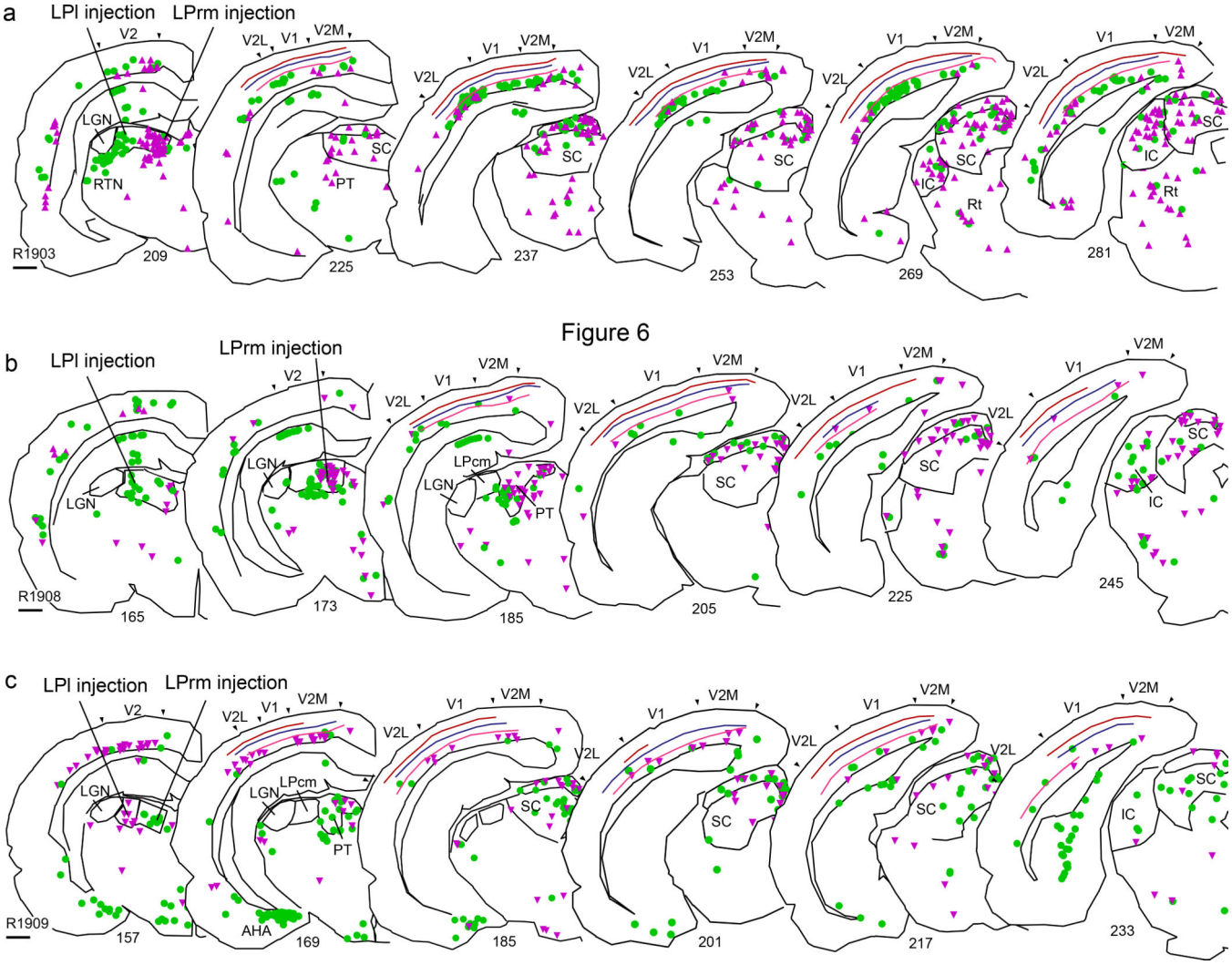

Figure 6.

Reconstructions of fluorescently labeled neurons identified following rabies injections in LPrm and LPl in three rats. Each LPl injection and each LPrm injection was targeted to the same stereotaxic coordinates and used the same volume, with the exception of rat R1908 (b), where more posterior LPrm was targeted to avoid a blood vessel. The superficial layers of the superior colliculus are demarcated. Magenta triangles indicate mCherry fluorescence, green circles indicate GFP. Borders between layer 3/4, 4/5, and 5/6 are shown. IC inferior colliculus, RTN reticular thalamic nucleus, PT pretectal nucleus, Rt reticular formation. AHA amygdalohippocampal area. Scale bars equal 1 mm.

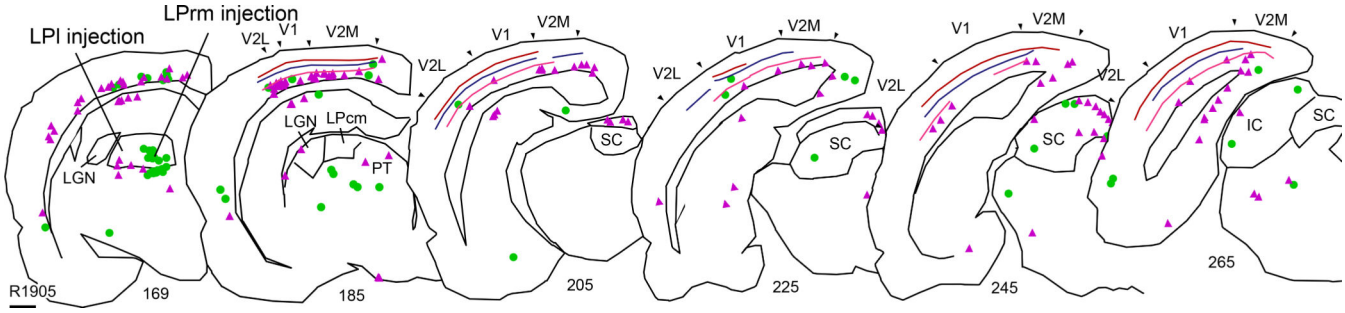

Figure 7.

Reconstruction of rat R1905, in which retrograde injections were made in the rostral portions of LPl and LPrm. Very little labeling is apparent in pretectum (PT) and superior colliculus (SC) following GFP virus injection into LPrm in this case (green circles). Injection of mCherry virus (magenta triangles) yielded similar results to previous injections. Borders between layer 3/4, 4/5, and 5/6 are shown. Scale bar equals 1 mm.

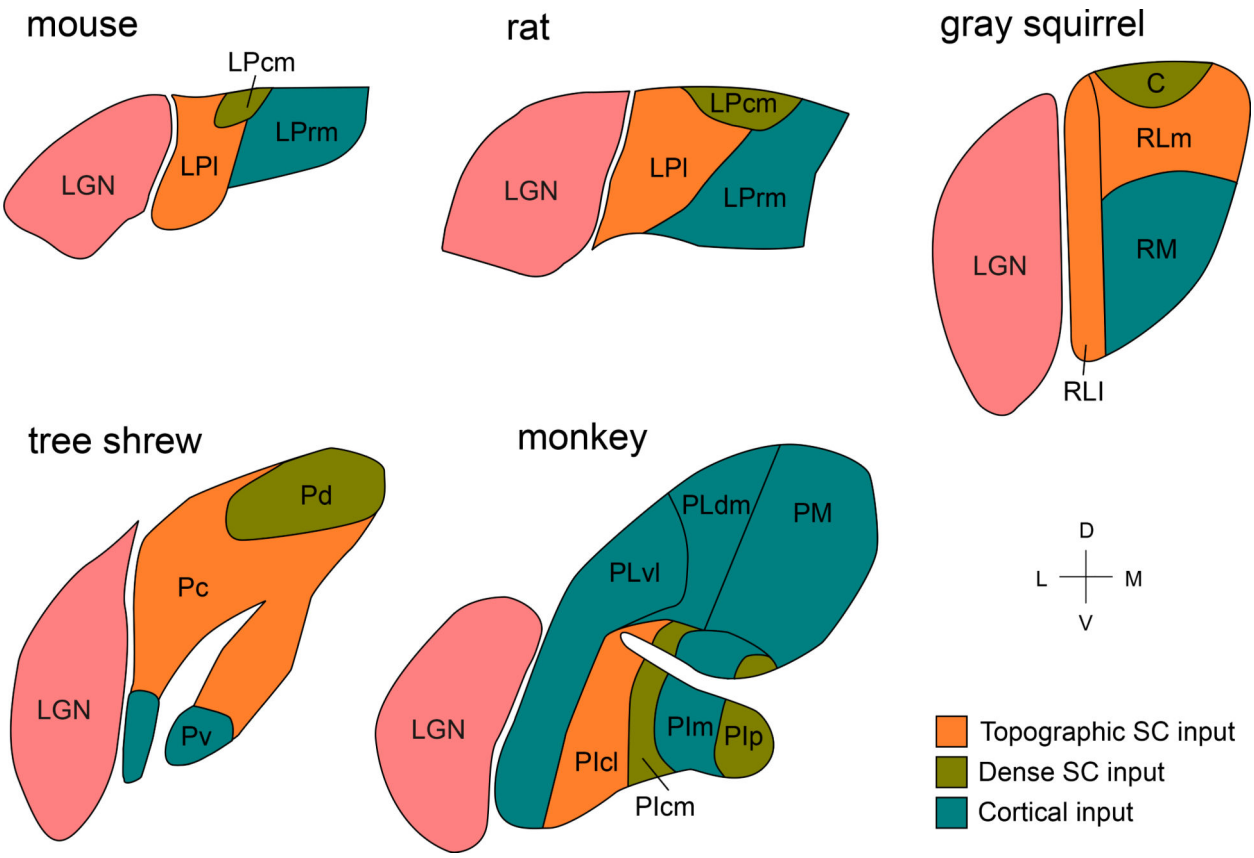

Figure 8.

Conserved pulvinar input scheme from SC and visual cortex across species. Schematic diagrams of the pulvinar in mouse, rat, gray squirrel, tree shrew, and monkey are shown. Areas with dense bilateral input from SC are shown in green, areas with ipsilateral SC input are shown in orange, and cortical recipient areas are shown in blue. Adapted from Lyon et al. (2003) and Zhou, Maire, et al. (2017).

Table 1.

Injection sites and total injection volume at each site for all cases. mCherry and GFP refer to mCherry and GFP modified rabies viruses.

Case	Virus	Inj site	Injection volume (uL)
R1630	mCherry	AL	1.2
R1703	mCherry	V1	3.6
	GFP	V1	3.6
R1802	mCherry	V1	2.4
	GFP	V1	2.4
R1803	GFP	LM	1.2
R1902	mCherry	AM	4.8
	GFP	PM	4.8
R1903	mCherry	LPrm	3.6
	GFP	LPl	3.6
R1905	mCherry	LPl	1.8
	GFP	LPrm	1.8
R1908	mCherry	LPrm	3.6
	GFP	LPl	3.6
R1909	mCherry	LPl	3.6
	GFP	LPrm	3.6

Table 2.

Percent of retrogradely labeled thalamic cells following cortical rabies virus injections.

Rat	Virus	Target	No of cells	LPrm	LPl	LPcm	LGN
R1703	GFP	V1 anterior	16	6	13	0	81
	mCherry	V1 posterior	21	0	19	0	81
R1802	mCherry	V1	34	6	9	6	79
	GFP	V1	26	4	8	4	85
			Mean	**4**	**12**	**2**	**82**
R1630	mCherry	V2L (AL)	19	11	63	11	16
R1803	GFP	V2L (LM)	15	7	53	13	27
R1902	mCherry	V2M (AM)	124	44	54	2	0
	GFP	V2M (PM)	61	41	46	3	10
			Mean	**26**	**54**	**7**	**13**
			Total Mean	**15**	**33**	**5**	**47**

Table 3.

Percent of retrogradely labeled cortical cells following LP injections

Rat		Target	No of cells	V1	V2	V1 Layer 5	V1 Layer 6	V2 Layer 5	V2 Layer 6
R1903	mCherry	LPrm	159	14	86	24	76	16	84
R1905	GFP	LPrm anterior	35	17	83	38	63	21	79
R1908	mCherry	LPrm	76	30	70	91	9	60	40
R1909	GFP	LPrm	74	31	69	17	83	28	72
			Mean	**23**	**77**	**51**	**49**	**32**	**68**
R1903	GFP	LPl	425	32	68	5	95	9	91
R1905	mCherry	LPl anterior	231	25	75	17	83	11	89
R1908	GFP	LPl	109	28	72	27	73	23	78
R1909	mCherry	LPl	131	35	65	18	82	13	87
			Mean	**30**	**70**	**17**	**83**	**14**	**86**
			Total Mean	**26**	**74**	**31**	**69**	**22**	**78**